.2

CONF-900772--2

BNL-45003

The e^+, e^- Background at RHIC Generated by Beam Crossing†

Mark J. Rhoades-Brown, T. Ludlam

The RHIC Project

Brookhaven National Laboratory

Associated Universities, Inc.

Upton, Long Island, New York 11973

BNL--45003

DE90 017203

J. Wu, C. Bottcher, M. Strayer

Physics Division

Oak Ridge National Laboratory

Oak Ridge, TN 37831

August 10, 1990

† Talk presented at July 1990 4th RHIC Workshop.

Introduction

At the Brookhaven Relativistic Heavy Ion Collider[1] (RHIC), fully stripped heavy ions will circulate in each of two rings up to beam energies of 250 (Z/A) GeV/u. During the beam crossing, the peripheral electromagnetic interaction between the heavy ions is sufficient to induce copious production of di-lepton pairs. These pairs are a potential source of background for the detectors at RHIC.

In this paper we discuss the expected number of e^+, e^-pairs, given the accepted initial luminosity value L of the collider. More importantly, we also calculate the differential cross sections for the angle, energy, rapidity and momentum distribution of the leptons. Using the luminosity L of the collider, these differential cross sections are normalized to the expected number of leptons per second. We restrict ourselves to e^+, e^-production, a discussion of $\mu^+\mu^-$ and $\tau^+\tau^-$ distributions will be published later. The results are presented for the expected worst case, namely $^{197}Au^{79+}$ions at a beam kinetic energy of 100 GeV/u. This is forseen to be the heaviest ion for high luminosity experiments at RHIC. We note for a given energy, the cross section for e^+, e^-production scales as Z^4, where Z is the atomic number of the ions.

The calculated cross sections correspond to a lepton energy or momentum range up to 1 GeV. For this range the differential cross section falls over many orders of magnitude, and should be adequate to estimate how many leptons will enter the RHIC detectors. On this note, it is expected that the calculations shown here will form the basis of a future peripheral collision event generator for RHIC. In this way, the final angular geometries of RHIC detectors can be used as input parameters to the event generator, thus enabling a selected binning for the differential distributions of the leptons.

Production rate of e^+, e^-pairs

For $^{197}Au^{79+}$beams at top RHIC energies, the total cross section σ_c for e^+, e^-production has been confidently calculated to be[2,3] 33Kb. This value of σ_c corresponds to the perturbative two photon diagram shown in Fig. 1, where this diagram has been evaluated exactly using Monte Carlo techniques[2], or via the analytic expression due to Racah[4]. The

remarkable agreement between these two approaches is shown in Fig. 2 for beam γ values spanning nearly four orders of magnitude.

For the $^{197}Au^{79+}$beam luminosity values at RHIC, the production rate of e^+, e^-pairs is given as $L\sigma_c$ sec^{-1}, where

$$L\sigma_c = 2 \times 10^{26} cm^{-2} sec^{-1} \times 33 \times 10^{-21} cm^2 \equiv 6.7 \times 10^6 sec^{-1}.$$

It is also important to note that at top RHIC energies for $^{197}Au^{79+}$beams, the perturbative calculation corresponding to Fig. 1 violates the unitary bound for the pair production S–matrix element. The amount by which the S–matrix element exceeds unity depends on the choice of impact parameter between the heavy ions. One estimate[5] for $^{197}Au^{79+}$beams at $\gamma = 100$, gives the probability for producing an e^+, e^-pair at an impact parameter of one Compton wavelength (386 fm) as 2.5. It seems clear that multiple pair production will play a role at RHIC, that is for top RHIC energies non–perturbative Q.E.D. effects such as multiple e^+, e^-pair production will be present. The exact nature of these higher order effects is still under investigation, and is one of controversy[3,5]. At this time it would seem that the number of pairs may be a few (3–5) times larger than the $\sim 10^7$ sec^{-1} value above[5,6].

Differential Cross Section for e^+, e^-production

In Figs. 3–12, the differential cross sections for the electrons produced from beam crossing are plotted as a function of various independent variables. The perturbative calculations were performed with a modified version of the Monte Carlo code[2] used to estimate the total cross section for e^+, e^-production. In all the following calculations, the differential cross sections have been scaled with the luminosity value L $\equiv 2 \times 10^{26}$ cm^{-2}sec^{-1} for $^{197}Au^{79+}$beams at RHIC. Thus, for example, the perpendicular momentum $p_\perp$ is rescaled as

$$\frac{d\sigma_c}{dp_\perp}(b/GeV) \rightarrow \frac{dN}{dp_\perp}(sec^{-1}GeV^{-1}) \equiv L\frac{d\sigma_c}{dp_\perp}(sec^{-1}GeV^{-1}),$$

where N is the number of pairs per second. Because of the problem of multiple pair production through higher order Q.E.D. effects, the distribution functions discussed in this section should be considered lower limits on N.

Figures 3–4 show the all important $dN/dp_\perp$ as a function of $p_\perp$ in GeV (velocity of light c put equal to 1). For the pair curve, $p_\perp$ is the perpendicular projection (relative to beam direction) of the total momentum of the produced pair. For the singles, $p_\perp$ is the perpendicular projection (relative to beam direction) of a single lepton momentum value.

The nuclear form factors play an important role in the transverse momentum differential cross sections. Figure 3 shows that the nuclear form factor severely attenuates the differential cross section for $p_\perp \geq 100$ MeV. This attenuation is very evident for the pair distribution. For values of $p_\perp < 100$ MeV, the nuclear form factor has a small effect on $dN/dp_\perp$, however for completeness the results shown in Fig. 4 were calculated with a nuclear form factor. The nuclear form factor used throughout this manuscript corresponds to a Fourier transform of a radial Woods–Saxon density distribution that was fitted to electron scattering data.[7]

Figures 3–4 show how soft the produced electrons are. As $p_\perp$ increases from 0 to 100 MeV, $dN/dp_\perp$ falls nearly six orders of magnitude for the pairs calculated including a nuclear form factor. In spite of the general rapid fall of in $dN/dp_\perp$, some care must be taken with any detector design for the absolute value of $dN/dp_\perp$ is still of considerable magnitude.

In Figs. 5–6, the differential cross sections $dN/dp_\parallel$ are plotted as a function of the longitudinal momentum $p_\parallel$. Once again for the pairs, $p_\parallel$ is the longitudinal projection (along the beam direction) of the total pair momentum, and for the singles $p_\parallel$ is the longitudinal projection of a single lepton. The nuclear form factor has been included in the calculations, but is of negligible importance for this variable. Of course, the curves are symmetric around $p_\parallel = 0$ for this variable. Analogous results in Figs. 7–8 show the differential cross section for the energy variable E.

The angular distributions of the pairs and singles are shown in Figs. 9–10. The angle θ is defined relative to the beam direction. The differential cross section $dN/d(\cos\theta)$ is symmetric with respect to $\theta = 90°$, and is independent of the azimuthal angle. The results show the leptons tend to travel in the forward (or backward) direction, but the total integrated cross section still has contributions for the approximate theta range $0 < \theta \leq 60°$.

The rapidity spectrum is shown in Fig. 11. It can be seen that beyond y = ± 4 units that dN/dy falls exponentially with increasing y.

Discussion

At relativistic energies, the Lorentz contracted Coulomb field between heavy ions in a collider will induce copious amounts of lepton pair production. In this note we have calculated differential cross sections for the produced e^+, e^-particles using exact Monte Carlo evaluation of the perturbative two photon diagram in Fig. 1.

There is some uncertainty in the exact number of pairs that will be produced, because traditional non–perturbative Q.E.D. violates unitarity bounds at RHIC energies. Work is continuing on this more fundamental problem of calculating and summing the Q.E.D. perturbation series.[8]

On a related note, some of the produced electrons (approximately 1 in 440 for $^{197}Au^{79+}$beams) can be captured in a K-orbital of the ion[9]. This mechanism will cause the ion to be lost from the beam, and hence reduce the overall beam lifetime. While reliable perturbative estimates have been made[9], work also continues on this important subject.

This research was sponsored by the Division of Nuclear Physics of the U.S. Department of Energy under contract No. DE–AC02– 76CH00016 with Brookhaven National Laboratory, under contract No. DE–AC05–84OR21400 with Martin Marietta Energy Systems, Inc.

REFERENCES

1 Conceptual Design of the Relativistic Heavy Ion Collider RHIC, May 1989, BNL 52195.

2 C. Bottcher and M. Strayer, Phys. Rev. D39, 1330 (1989).
M. Strayer, invited talk, presented at the workshop "Can RHIC be used to test Q.E.D.?", Brookhaven National Laboratory, Upton, New York, April 1990, BNL 52247.

3 S. Brodsky, invited talk, presented at the workshop "Can RHIC be used to test Q.E.D.?", Brookhaven National Laboratory, Upton, New York, April 1990, BNL 52247.

4 G. Racah, Nuovo Cimento 14, 70 (1937).

5 G. Baur, invited talk, presented at the workshop "Can RHIC be used to test Q.E.D.?", Brookhaven National Laboratory, Upton, New York, April 1990, BNL 52247.

6 M. Fatyga, M.J. Rhoades-Brown, M. Tannenbaum, workshop summary, presented at the workshop "Can RHIC be used to test Q.E.D.?", Brookhaven National Laboratory, Upton, New York, April 1990, BNL 52247.

7 R.C. Barrett and D.F. Jackson, "Nuclear Sizes and Structure", Oxford University Press, 1975.

8 C. Bottcher, invited talk, presented at the workshop "Can RHIC be used to test Q.E.D.?", Brookhaven National Laboratory, Upton, New York, April 1990, BNL 52247.

9 M.J. Rhoades-Brown, C. Bottcher, M. Strayer, Phys. Rev. A40, 2831 (1989).

FIGURE CAPTIONS

Fig. 1 Schematic representation of perturbative two photon diagram, including exchange term.

Fig. 2 Comparison of full Monte Carlo evaluated cross section and Racah formula as function of beam γ value. σ_0 is a scaling parameter that takes the value 165b for $^{197}Au^{79+}$beams.

Fig. 3 Comparison of $dN/dp_\perp$ as function of $p_\perp$, for both pairs and singles, with and without the nuclear form factor.

Fig. 4 Same as Fig. 3, but for smaller $p_\perp$ scale. Both pairs and singles include the nuclear form factor.

Fig. 5 Plot of $dN/dp_\parallel$ as function of $p_\parallel$, for both pairs and singles, with nuclear form factor.

Fig. 6 Same as Fig. 5, but for smaller $p_\parallel$ range.

Fig. 7 Plot of dN/dE as function of energy E, for both pairs and singles, with nuclear form factor.

Fig. 8 Same as Fig. 7, but for smaller E range.

Fig. 9 Plot of $dN/d(\cos\theta)$ as function of opening angle θ, for both pairs and singles, with nuclear form factor.

Fig. 10 Same as Fig. 9, but for smaller θ range.

Fig. 11 Plot of dN/dy as function of rapidity y, for both pairs and singles, with nuclear form factor.

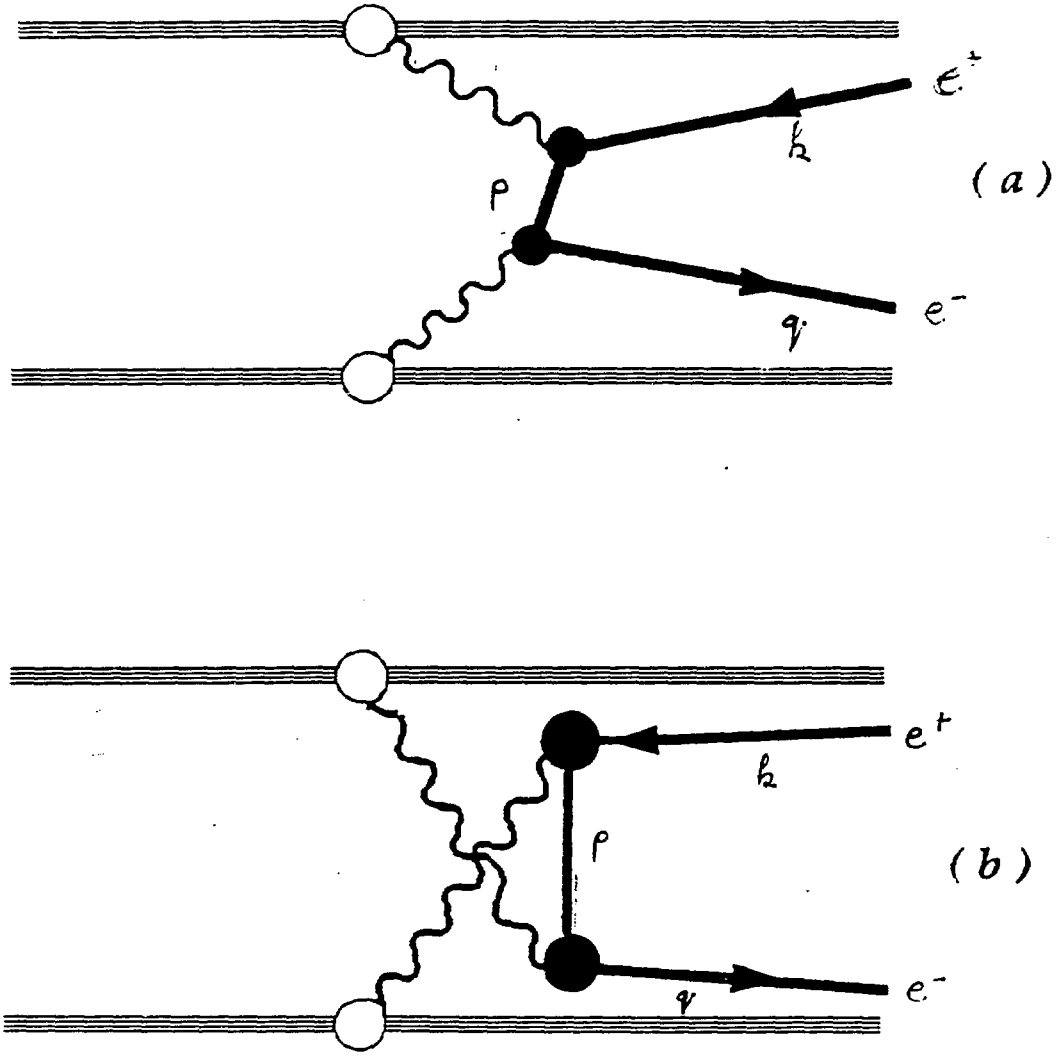

Fig. 1

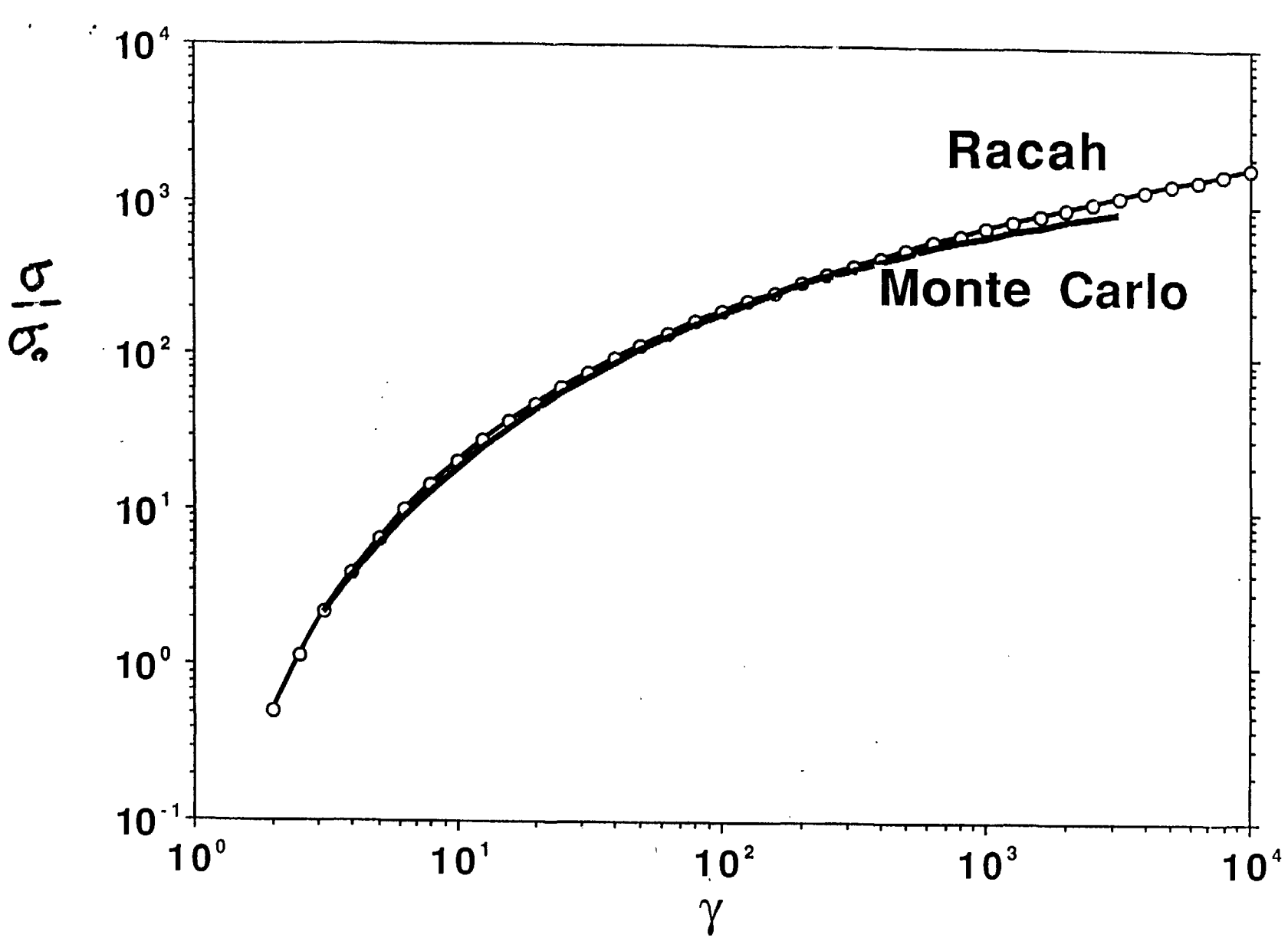
10^4
10^3
10^2
10^1
10^0
10^{-1}
σ_0/σ
Racah
Monte Carlo
10^0
10^1
10^2
10^3
10^4
γ

Fig. 2

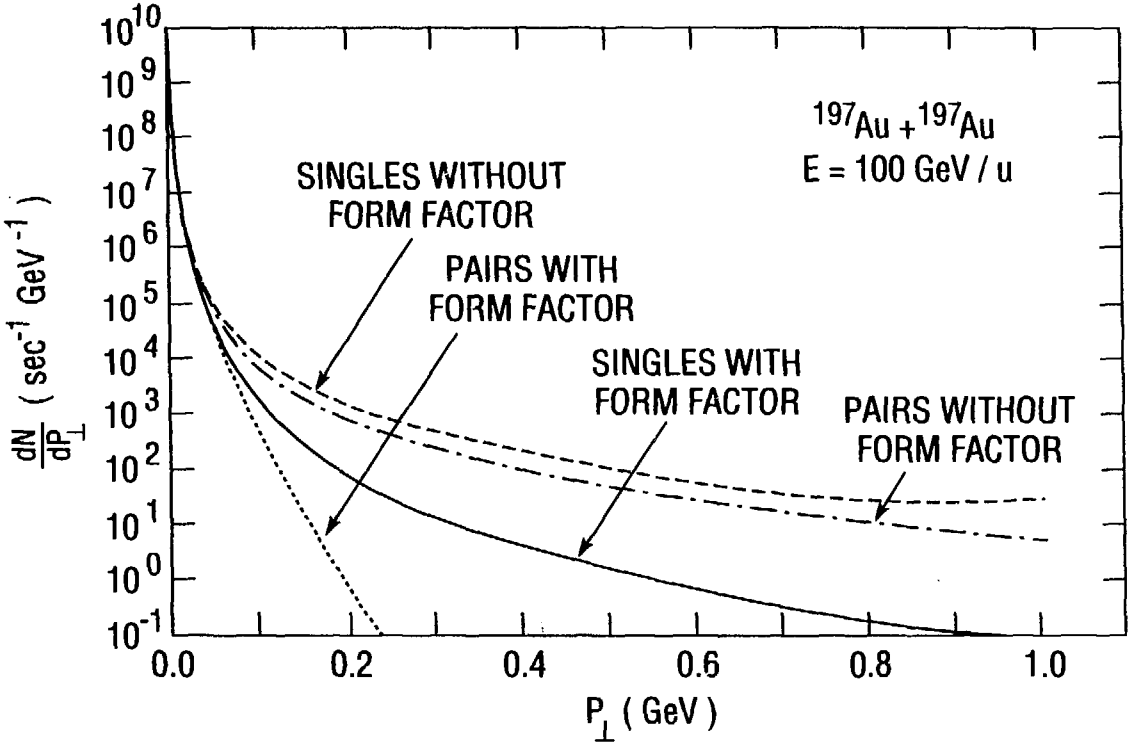
10^{10}
10^{9}
10^{8}
10^{7}
10^{6}
10^{5}
10^{4}
10^{3}
10^{2}
10^{1}
10^{0}
10^{-1}
$\frac{dN}{dP_\perp}$ (sec^{-1} GeV^{-1})
$^{197}Au + ^{197}Au$
E = 100 GeV / u
SINGLES WITHOUT FORM FACTOR
PAIRS WITH FORM FACTOR
SINGLES WITH FORM FACTOR
PAIRS WITHOUT FORM FACTOR
0.0
0.2
0.4
0.6
0.8
1.0
$P_\perp$ (GeV)

Fig. 3

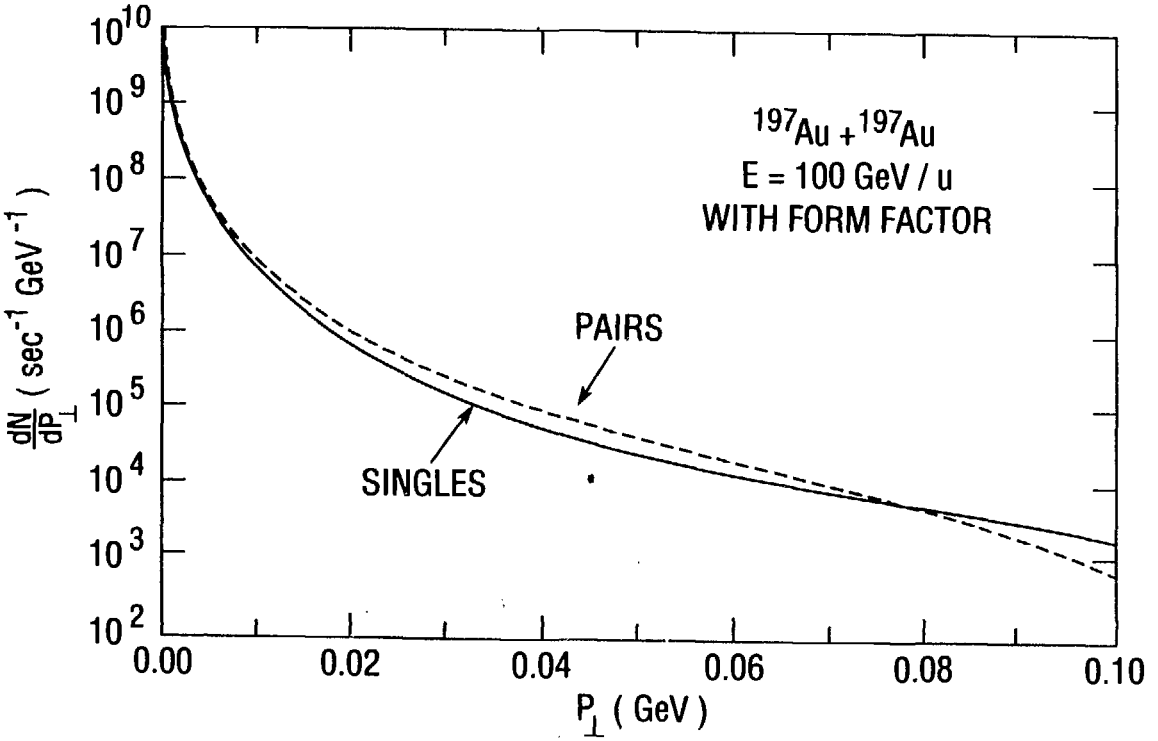
10^{10}
10^{9}
10^{8}
10^{7}
10^{6}
10^{5}
10^{4}
10^{3}
10^{2}
$\frac{dN}{dP_\perp}$ (sec^{-1} GeV^{-1})
$^{197}Au + ^{197}Au$
E = 100 GeV / u
WITH FORM FACTOR
PAIRS
SINGLES
0.00
0.02
0.04
0.06
0.08
0.10
$P_\perp$ (GeV)

Fig. 4

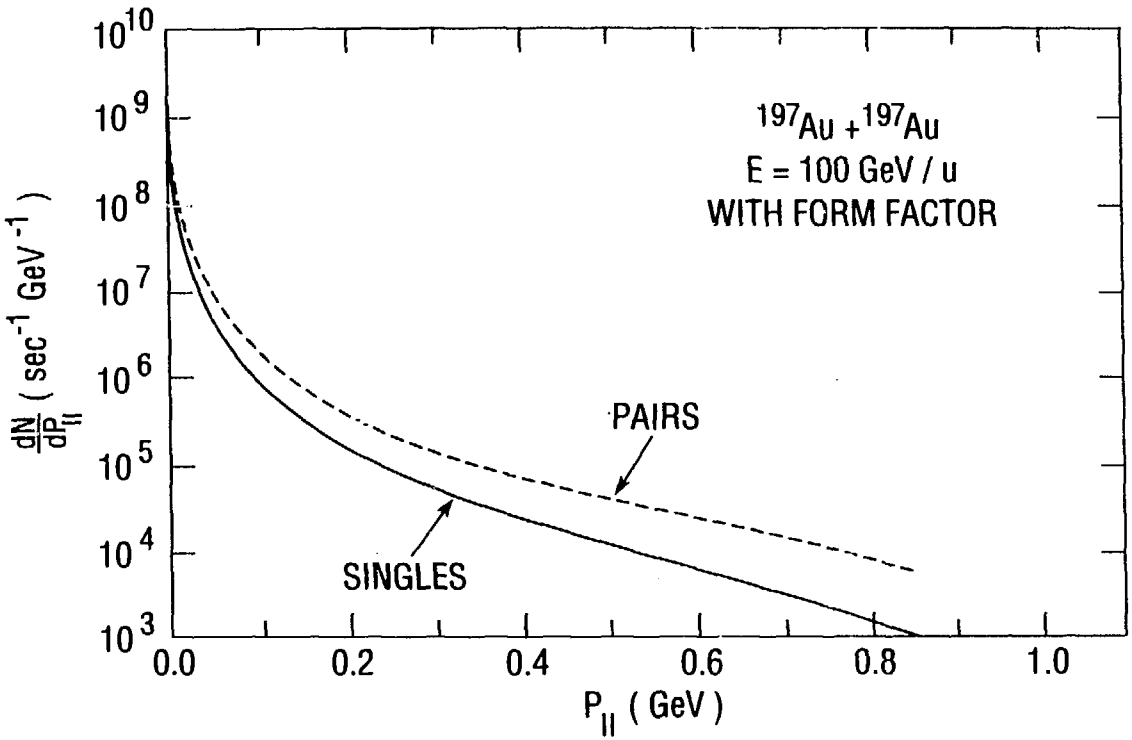
10^{10}
10^{9}
10^{8}
10^{7}
10^{6}
10^{5}
10^{4}
10^{3}
$\frac{dN}{dP_{ll}}$ (sec^{-1} GeV^{-1})
$^{197}Au + ^{197}Au$
E = 100 GeV / u
WITH FORM FACTOR
PAIRS
SINGLES
0.0
0.2
0.4
0.6
0.8
1.0
P_{ll} (GeV)

Fig. 5

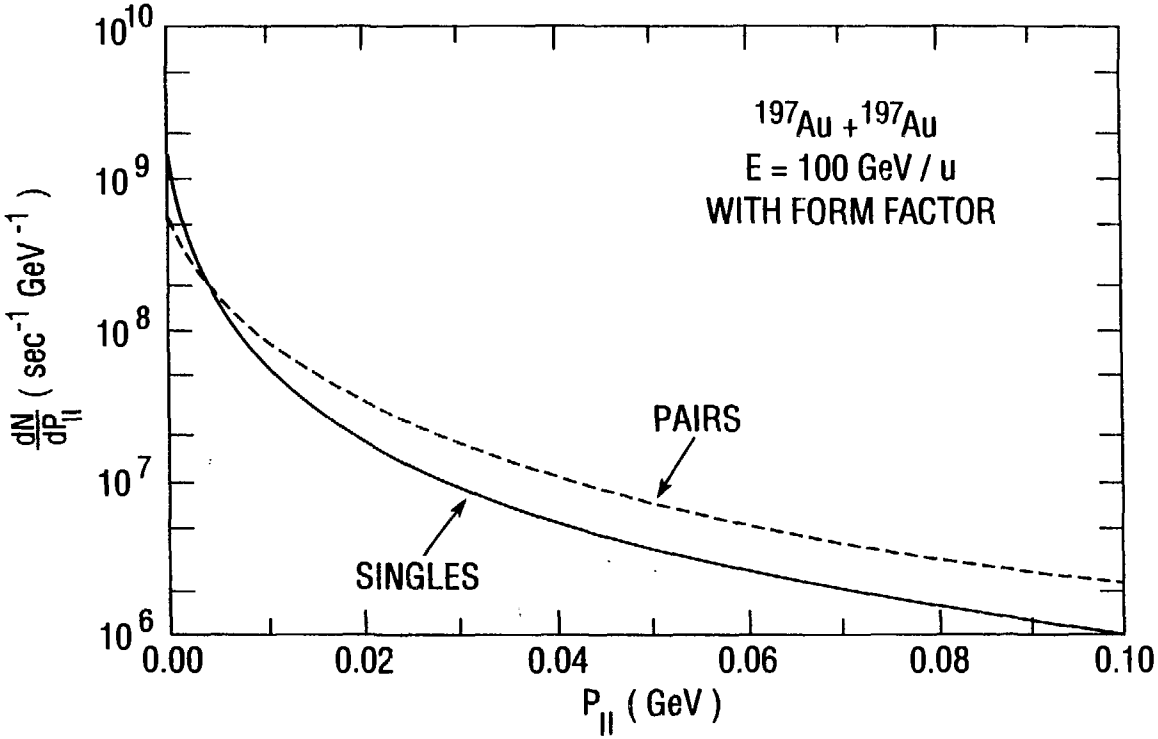
10^{10}
10^{9}
10^{8}
10^{7}
10^{6}
$\frac{dN}{dP_{ll}}$ (sec^{-1} GeV^{-1})
$^{197}Au + ^{197}Au$
E = 100 GeV / u
WITH FORM FACTOR
PAIRS
SINGLES
0.00
0.02
0.04
0.06
0.08
0.10
P_{ll} (GeV)

Fig. 6

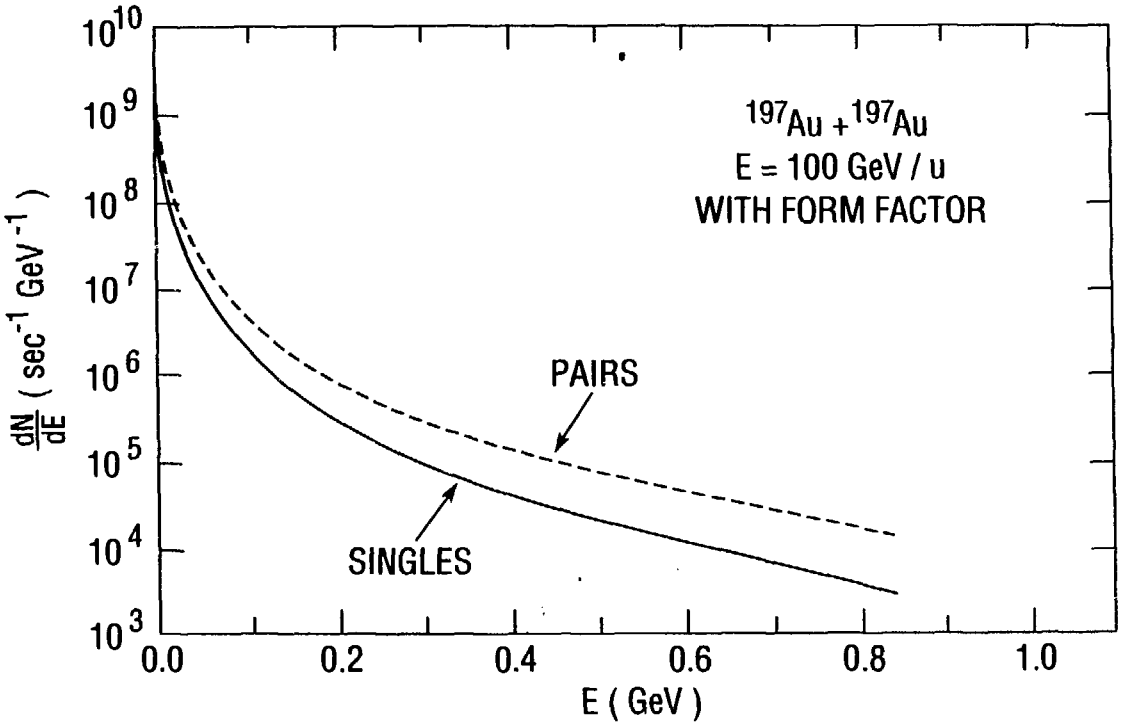
10^{10}
10^{9}
10^{8}
10^{7}
10^{6}
10^{5}
10^{4}
10^{3}
$\frac{dN}{dE}$ (sec^{-1} GeV^{-1})
$^{197}Au + ^{197}Au$
E = 100 GeV / u
WITH FORM FACTOR
PAIRS
SINGLES
0.0
0.2
0.4
0.6
0.8
1.0
E (GeV)

Fig. 7

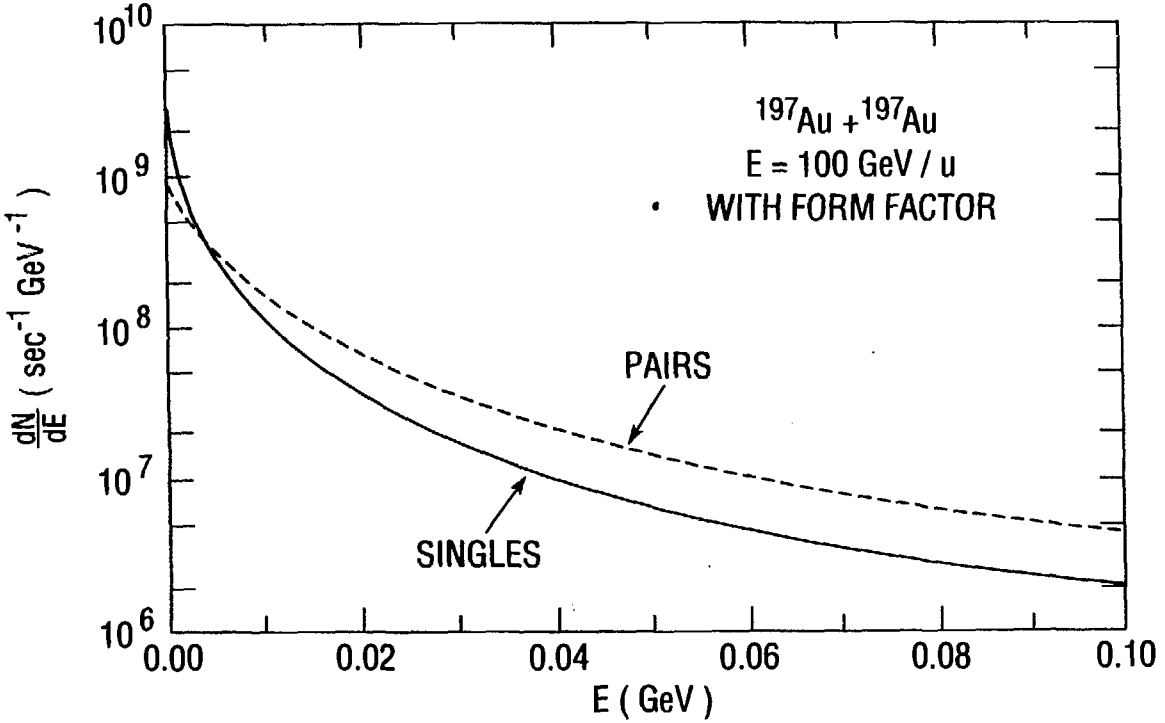
10^{10}
10^{9}
10^{8}
10^{7}
10^{6}
$\frac{dN}{dE}$ (sec^{-1} GeV^{-1})
$^{197}Au + ^{197}Au$
E = 100 GeV / u
WITH FORM FACTOR
PAIRS
SINGLES
0.00
0.02
0.04
0.06
0.08
0.10
E (GeV)

Fig. 8

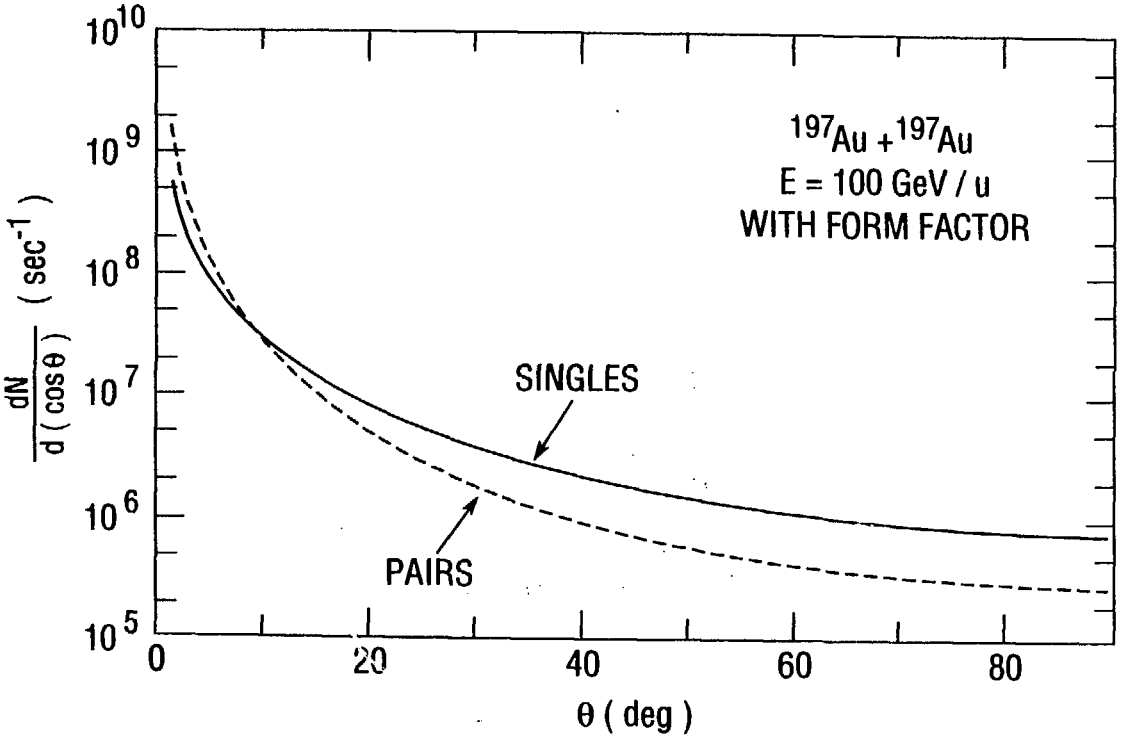
10^{10}
10^{9}
10^{8}
10^{7}
10^{6}
10^{5}
$\frac{dN}{d(\cos\theta)}$ (sec^{-1})
$^{197}Au + ^{197}Au$
E = 100 GeV / u
WITH FORM FACTOR
SINGLES
PAIRS
0
20
40
60
80
θ (deg)

Fig. 9

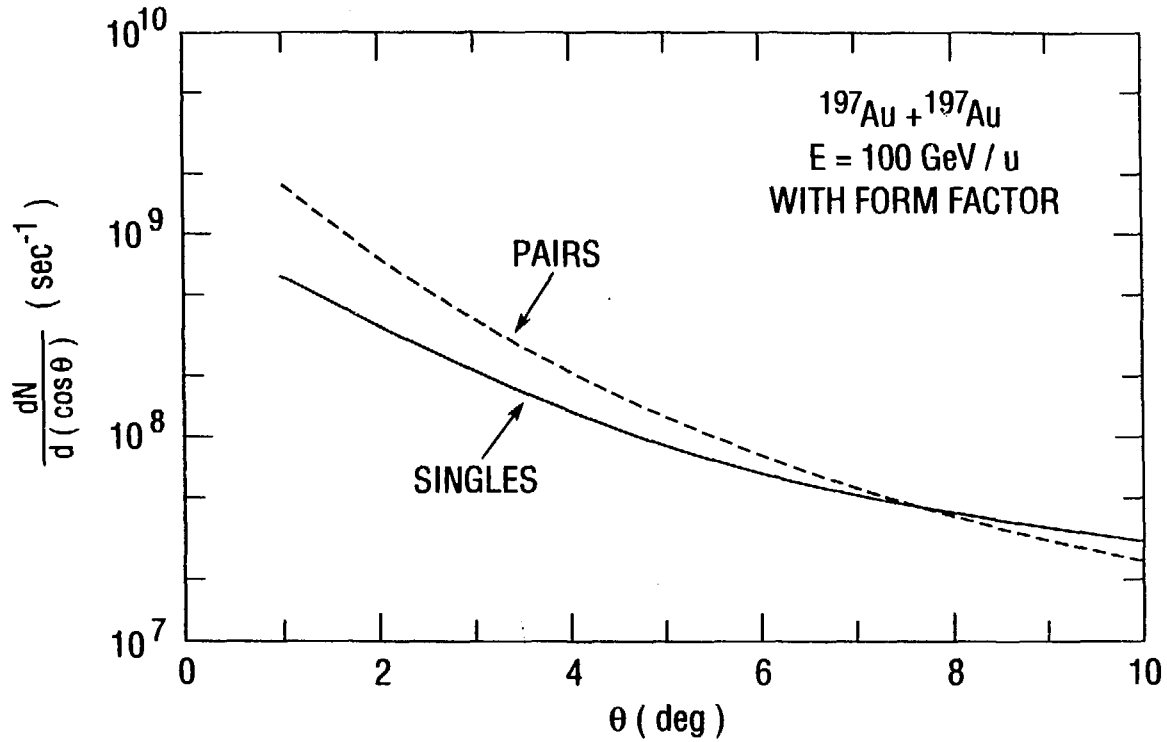
10^{10}
10^{9}
10^{8}
10^{7}
$\frac{dN}{d(\cos\theta)}$ (sec^{-1})
$^{197}Au + ^{197}Au$
E = 100 GeV / u
WITH FORM FACTOR
PAIRS
SINGLES
0
2
4
6
8
10
θ (deg)

Fig. 10

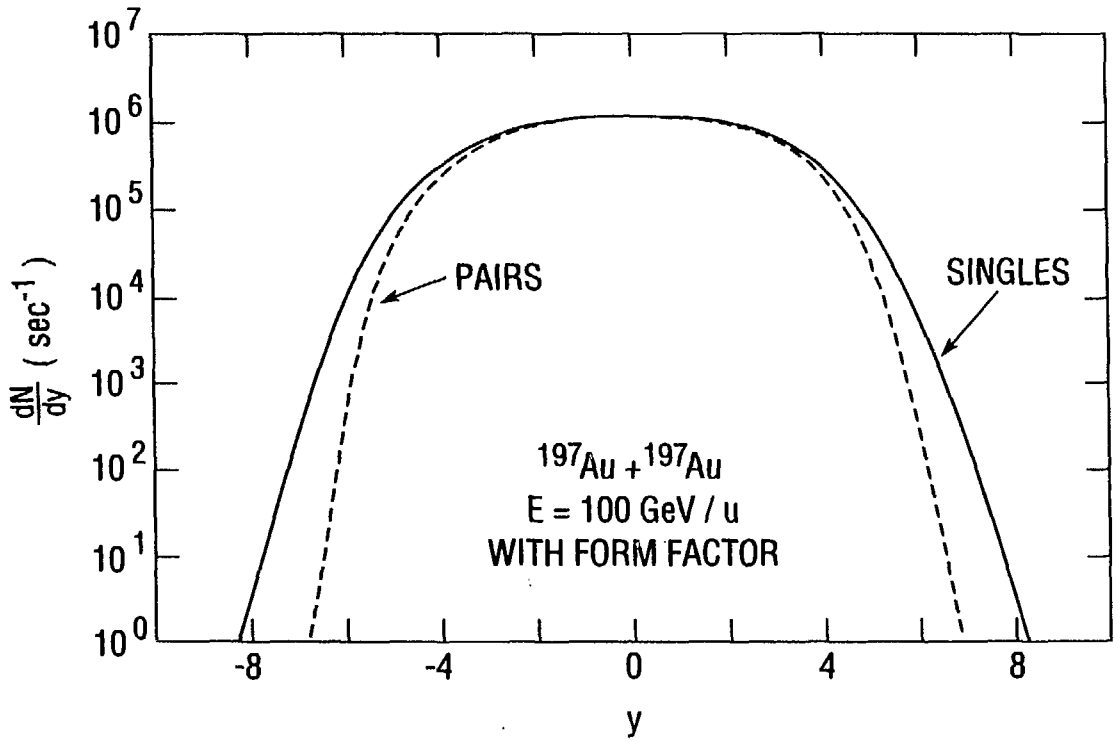
10^7
10^6
10^5
10^4
10^3
10^2
10^1
10^0
$\frac{dN}{dy}$ (sec^{-1})
PAIRS
SINGLES
$^{197}Au + ^{197}Au$
E = 100 GeV / u
WITH FORM FACTOR
-8
-4
0
4
8
y

Fig. 11